ELSEVIER

Journal of Organometallic Chemistry 637–639 (2001) 172–181

Journal of Organometallic Chemistry

www.elsevier.com/locate/jorganchem

Bonding in 'closed,' open, and half-open ferrocenes: new insight from structural and Mössbauer spectroscopic studies

Rehan Basta [a], David R. Wilson [a,1], Huairang Ma [a], Atta M. Arif [a], Rolfe H. Herber [b,*], Richard D. Ernst [a,*]

[a] *Department of Chemistry, University of Utah, 315 S, 1400 E, Room 2020, Salt Lake City, UT 84112-0850, USA*
[b] *Racah Institute of Physics, The Hebrew University of Jerusalem, 91904 Jerusalem, Israel*

Received 20 December 2000; received in revised form 22 February 2001; accepted 22 February 2001

Abstract

A 17 electron edge-bridged open metallocene, bis(6,6-dimethylcyclohexadienyl)iron cation, which had previously been observed electrochemically, has been isolated and characterized. Mössbauer spectroscopic data have been obtained for this compound, and for various neutral 18 electron open, half-open, and 'closed' ferrocenes, and are in accord with the previous indications that much greater metal–ligand orbital mixing occurs for pentadienyl, as opposed to cyclopentadienyl, ligands. Pertinent structural data have also been obtained for $Fe(C_5H_5)(2,4\text{-}C_7H_{11})$ and $Fe(c\text{-}C_7H_9)_2$ (C_7H_{11} = dimethylpentadienyl; $c\text{-}C_7H_9$ = cycloheptadienyl) in order to aid in comparisons between metal–pentadienyl and metal–cyclopentadienyl bonding. © 2001 Elsevier Science B.V. All rights reserved.

Keywords: Metallocenes; Mössbauer spectroscopy; Ferrocene half-sandwich

1. Introduction

The discovery of ferrocene (**1**) and the elucidation of its structure was one of those rare events that revolutionized the entire field of organometallic chemistry, and after a period of 50 years, has led to many practical applications for metal cyclopentadienyl (Cp) complexes, including very large scale polymerization processes [1], applications in organic synthesis [2], as well as more specialized applications (e.g. low dimensional conductors and superconductors, redox tunable auxiliaries in molecular composites, luminescent, fluorescent, and photoreflective materials [3], in addition to the use of ferrocenes themselves as burn enhancers [4]). The importance of the discovery of ferrocene, and related π-complexes, was recognized appropriately by the award of the 1973 Nobel Prize to Professors Fischer and Wilkinson [5].

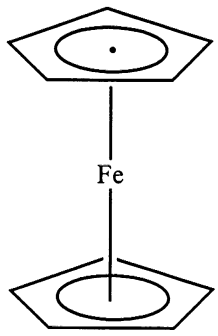

1

Much of the interest in ferrocene derives from its high thermal stability, and the strong bonding generally found between transition metal centers and the Cp ligand, which can be exemplified by the existence of a whole series of thermally stable metallocenes from the 15 electron vanadocene to the 20 electron nickelocene [6]. As a result, Cp is often described as a 'stabilizing ligand.' Recently it has become evident that open pentadienyl ligands, e.g. C_5H_7 (**2**) and $2,4\text{-}C_7H_{11}$ (**3**), can be even more strongly bound ligands than Cp [7], and a

* Corresponding authors. Tel.: +1-801-581-6681; fax: +1-801-581-8433 (R.D.E.).
E-mail addresses: herber@vms.huji.ac.il (R.H. Herber), ernst@chem.utah.edu (R.D. Ernst).
[1] Present address. The Dow Chemical Company, 1776 Building, Chemical Sciences Capability, Midland, MI 48674, USA.

PII: S0022-328X(01)00901-9

variety of open (**4**) and half-open (**5**) metallocenes can be isolated [8]. Since the π-molecular orbitals of pentadienyl anions in the U conformation are quite analogous to those of Cp [9], it has become of interest to probe the electronic natures of metal–pentadienyl interactions relative to those of their more familiar Cp counterparts. As Mössbauer spectroscopy yields significant information pertaining to the populations of metal-based orbitals, it provides substantial, important information on the relative extents of metal–ligand bonding interactions, thereby aiding in the efforts to gain a better understanding of open versus 'closed' pentadienyl ligands [10]. Moreover, in a historical context it is appropriate to note that ferrocene was the first organometallic compound to which ^{57}Fe Mössbauer spectroscopy was applied in the elucidation of the electronic environment of the metal atom. Herein we report Mössbauer spectroscopic data for various open, 'closed,' and half-open ferrocenes, as well as pertinent structural studies to assist in spectroscopic correlations and in bonding comparisons.

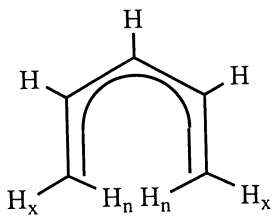

2

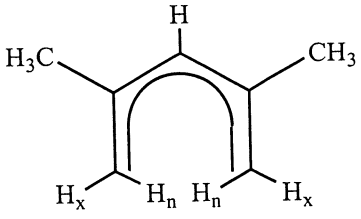

3

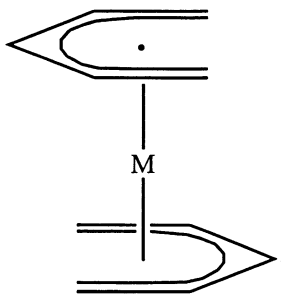

4

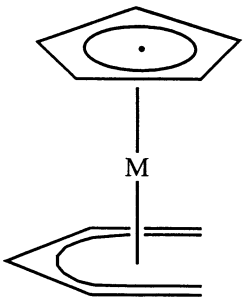

5

2. Results and discussion

2.1. Synthetic and structural data

The syntheses of the pentadienyl, 6,6-dmch (**6**), *c*-C_7H_9 (**7**), and *c*-C_8H_{11} (**8**) compounds studied here have generally been described previously [11], although in the case of Fe(*c*-C_7H_9)$_2$ [12], a new and more straightforward route utilizing the cycloheptadienyl anion was utilized, similar to the routes previously developed for its 6,6-dmch [13] and *c*-C_8H_{11} [14] analogues (dmch = dimethylcyclohexadienyl; *c*-C_7H_9 = cycloheptadienyl; *c*-C_8H_{11} = cyclooctadienyl). Notably, reversible electrochemical oxidation of the Fe(6,6-dmch)$_2$ complex had been reported by DiMauro and Wolczanski [15], and subsequent studies by LeSuer and Geiger have revealed the cation to be fairly stable in solution even at room temperature [16]. As a result, we have found it possible to isolate the cation as a tetraphenylborate salt. The stability of this cation is quite remarkable compared to other 17 electron open ferrocene cations [17], which could only be reversibly generated electrochemically using rapid scan rates at low temperatures. Thus, Fe(6,6-dmch)$_2^+$ actually appears to be the first clear example of an isolable 17 electron open metallocene, although DiMauro and Wolczanski have provided some evidence for the existence of Mn(6,6-dmch)$_2$ [13].

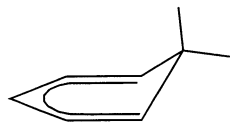

6

7

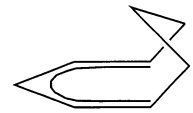

8

Although structural comparisons between ferrocene and various open ferrocenes have been made [8], such comparisons suffer from complications due to the differing symmetries and steric environments. These complications are nicely removed, however, in a half-open ferrocene complex such as Fe(C_5H_5)(2,4-C_7H_{11}), which then allows for direct and more valid comparisons to be made between the two ligands. As a result, a structural determination of this complex was undertaken. The solid state structure of Fe(C_5H_5)(2,4-C_7H_{11}) is consistent with the spectroscopic data (see Section 4), and is presented in Fig. 1, while pertinent bonding parameters are listed in Table 1. The molecule lies on a crystallographic mirror plane, resulting in an ideally eclipsed conformation (**9**) as opposed to the staggered alternative (**10**). There is, however, significant thermal motion associated with the C_5H_5 ligand, and it is therefore possible that the ground state conformation might actually not quite be eclipsed, leading to a superposition of two slightly staggered images in the solid state. As in the case of ferrocene, it must be expected that any difference in energy for these conformations should be rather small [18].

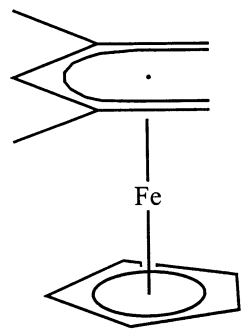

9

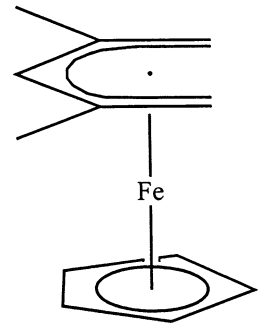

10

For the C_5H_5 ligand in **9**, one finds an average Fe–C distance of 2.063(5) Å, indistinguishable from that of 2.064(3) Å found for ferrocene by gas phase electron diffraction [19]. However, it is possible that the value in **9** could suffer a slight systematic shortening due to librational effects. For the pentadienyl ligand, there are modest differences in the Fe–C(1,2,3) distances, following a similar trend as in $Fe(2,4\text{-}C_7H_{11})_2$ (**11**), in which the formally uncharged (2,4) positions are closest to Fe, while the terminal (1,5) positions are farthest. The overall average Fe–C distance for the $2,4\text{-}C_7H_{11}$ ligand in **9** is 2.060(10,1) Å [20], significantly shorter than the average of 2.089 Å for $Fe(2,4\text{-}C_7H_{11})_2$ [21]. The lengthening of the Fe–C bonds in **11** has been attributed to the appreciable steric crowding that results from the long C1–C1′ separation for the $2,4\text{-}C_7H_{11}$ ligand (2.746 Å for **9** and 2.785(5) Å for **11**), which then requires a much closer approach of the ligand plane to the metal center (cf. 1.420 Å for $2,4\text{-}C_7H_{11}$ versus 1.687 Å for C_5H_5 in **9**). Additionally, in **11** there could be greater electronic competition between the two $2,4\text{-}C_7H_{11}$ ligands, which generally appear to be significantly stronger accepting ligands than C_5H_5 [10].

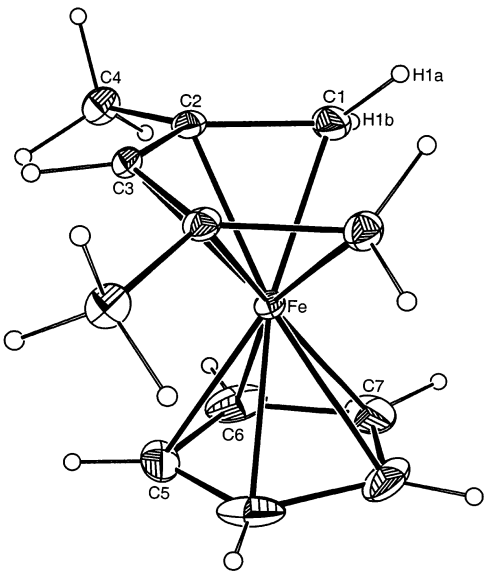

Fig. 1. Perspective view of the half-open ferrocene, $Fe(C_5H_5)(2,4\text{-}C_7H_{11})$.

Table 1
Bonding parameters for $Fe(C_5H_5)(2,4\text{-}C_7H_{11})$

Bond length (Å)			
Fe–C(1)	2.076(1)	C(1)–C(2)	1.424(2)
Fe–C(2)	2.045(1)	C(2)–C(3)	1.425(2)
Fe–C(3)	2.059(2)	C(2)–C(4)	1.511(2)
Fe–C(5)	2.059(2)	C(5)–C(6)	1.406(3)
Fe–C(6)	2.057(2)	C(6)–C(7)	1.398(3)
Fe–C(7)	2.071(2)	C(7)–C(7′)	1.39(4)
Bond angles (°)			
C(1)–C(2)–C(3)	121.37(13)	C(5)–C(6)–C(7)	108.2(2)
C(1)–C(2)–C(4)	120.63(13)	C(6)–C(7)–C(7′)	108.3(1)
C(2)–C(3)–C(2′)	125.37(17)	C(6)–C(5)–C(6′)	106.9(2)
C(3)–C(2)–C(4)	117.54(12)		

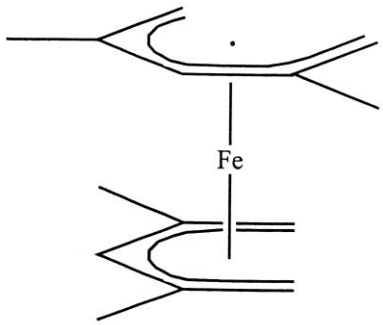

11

Several additional observations can also be made concerning the ligand planes. On average, the C_5H_5 substituents tilt down toward the iron center by 2.4°, close to the value of 3.7(9)° observed for ferrocene [19]. The reason for the tilt has been proposed to be an attempt of the ligand to improve orbital overlap with the relatively small iron center (**12**). On this basis one would then expect to observe even greater tilts for the $2,4\text{-}C_7H_{11}$ substituents, and indeed this is observed. The values for the 'downward oriented' C(1–3) substituents are, respectively, 17.6, 12.3, and 6.8°. For the internal (endo) substituents on C(1), the tilt is 46.2° in the opposite direction. The much greater tilt here could arise from an attempt to rehybridize the orbitals on C1 more toward sp^3, and to an attempt to reduce steric interactions between the two opposing substituents (H_n/H_n in **2** or **3**) [21,22]. The greater upward tilt of H_n would then either initiate or at least be accompanied by a significant downward tilt of H_x, and one then observes lesser degrees of tilting as one moves to C2 and C3. Finally, there is a tilt of 6.6(1)° between the two ligand planes, which can be compared to the value of 15.0° for **11**.

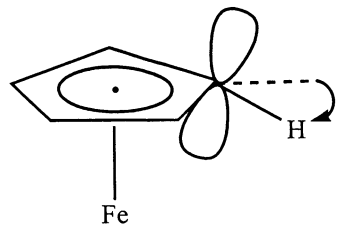

12

In order to learn more about the bonding in the edge-bridged analogues, a single crystal diffraction study of $Fe(c\text{-}C_7H_9)_2$ was carried out. Quite unusually, but not without precedent, four independent molecules

Table 2
Bonding parameters for Fe(c-C_7H_9)$_2$

		A	B	C
Bond length (Å)				
Fe–C(1)	2.071(2)	2.077(2)	2.057(2)	2.072(2)
Fe–C(2)	2.038(2)	2.041(2)	2.039(2)	2.037(2)
Fe–C(3)	2.064(2)	2.067(2)	2.066(2)	2.072(2)
Fe–C(4)	2.038(2)	2.036(2)	2.027(2)	2.038(2)
Fe–C(5)	2.126(2)	2.128(2)	2.113(2)	2.126(2)
Fe–C(8)	2.070(2)	2.073(2)	2.052(2)	2.074(2)
Fe–C(9)	2.041(2)	2.044(2)	2.042(2)	2.044(2)
Fe–C(10)	2.071(2)	2.066(2)	2.072(2)	2.065(2)
Fe–C(11)	2.039(2)	2.038(2)	2.033(2)	2.037(2)
Fe–C(12)	2.126(2)	2.128(2)	2.109(2)	2.128(2)
C(1)–C(2)	1.418(3)	1.413(3)	1.416(4)	1.421(3)
C(2)–C(3)	1.416(4)	1.419(3)	1.397(5)	1.419(3)
C(3)–C(4)	1.395(4)	1.404(3)	1.378(5)	1.408(3)
C(4)–C(5)	1.393(3)	1.404(3)	1.390(4)	1.404(3)
C(8)–C(9)	1.430(3)	1.416(3)	1.411(3)	1.418(3)
C(9)–C(10)	1.408(3)	1.413(4)	1.410(3)	1.417(3)
C(10)–C(11)	1.403(3)	1.396(3)	1.386(4)	1.407(3)
C(11)–C(12)	1.398(3)	1.407(3)	1.389(4)	1.402(3)
Bond angles (°)				
C(1)–C(2)–C(3)	126.6(2)	126.4(2)	125.9(2)	126.7(2)
C(2)–C(3)–C(4)	122.8(2)	122.7(2)	123.2(2)	122.4(2)
C(3)–C(4)–C(5)	119.2(2)	119.8(2)	120.0(3)	119.5(2)
C(8)–C(9)–C(10)	126.9(2)	126.5(2)	125.9(2)	126.2(2)
C(9)–C(10)–C(11)	122.8(2)	123.0(2)	123.0(2)	122.9(2)
C(10)–C(11)–C(12)	119.1(2)	119.6(2)	119.6(2)	119.2(2)

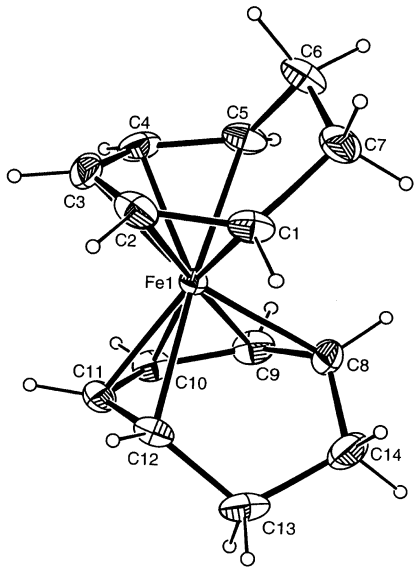

Fig. 2. Solid state structure of Fe(c-C_7H_9)$_2$. While only one of the four independent molecules is shown, the parameters of the other three are similar.

were contained in the triclinic unit cell. However, a close examination revealed that the structural parameters for these molecules were nearly indistinguishable (Table 2), and thus solid state packing effects appear to be relatively minimal. The one exception was for the third molecule (carbon atoms designated with B's), for which a number of parameters (e.g. Fe–C(1,4,5)) showed clear deviations from the values found in the other three molecules. That the deviating parameters could be considered less reliable can be supported by an examination of thermal parameters for the various C(1–5) atoms. The U values for these atoms in the three similar molecules range from 28(1) to 50(1), while in the unique molecule these range from 42(1) to 70(1). Therefore, in the subsequent discussion, the average values quoted for Fe(c-C_7H_9)$_2$ will be derived only from the three similar molecules.

To begin with, the molecule is found to adopt a nearly *gauche*-eclipsed conformation (**13**, Fig. 2), having a conformation angle of 53.9°, close to the ideal value of 60° relative to a *syn*-eclipsed structure (0°, **14**). As the conformation angles for non-edge bridged open ferrocenes have been found to be much closer to 60° [21,23], the small deviation here may be attributed to the presence of the C_2H_4 bridge, which leads to a relatively short C(1–5) separation, 2.715 Å (cf. 2.785 Å for Fe(2,4-C_7H_{11})$_2$, conformation angle 59.7°, and 2.706 Å for Fe(2,3,4-C_8H_{13})$_2$, conformation angle 55.1°). The relative Fe–C bond distances (Fe–C(1,8), C(2,9), C(3,10), C(4,11), C(5,12), respectively: 2.068(9), 2.041(3), 2.068(3), 2.036(4), and 2.123(8) Å) follow a pattern similar to those observed for other open ferrocenes, with the shortest distances being found for the formally uncharged carbon atoms in the 2 and 4 positions [21,23].

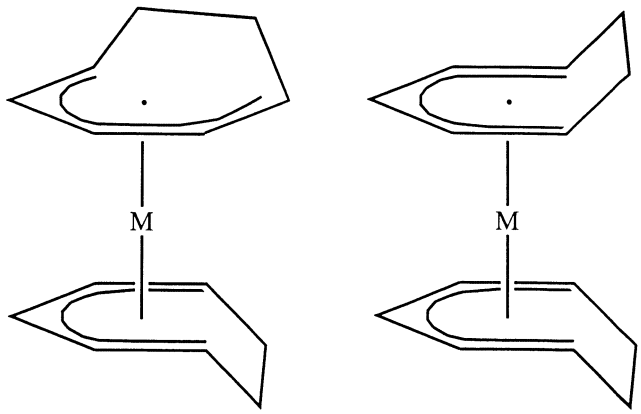

13 **14**

The dienyl fragments are not quite planar, with the carbon atom deviations ranging from an average of −0.064 Å for the C(5,12) atoms to an average of 0.086 Å for the C(4,11) atoms, a positive deviation reflecting a tilt toward the Fe center. However, the average C(1–4) and C(8–11) torsion angle is 1.8°, while that for the C(2–5) and C(9–12) fragments is 13.1°, reflecting a

deviation of the C(5,12) atoms out of the plane, away from the iron center and the opposing dienyl ligand. This is consistent with the longest Fe–C bonds involving C(5) and C(12), and may in part reflect the fact that C(5,12) engage in near-eclipsing interactions with the other dienyl ligand whereas C(1,8) reside by the other ligands' open edges. Related to these parameters is the tilt between the two dienyl ligands, which averages 13.9°.

However, the near planarity of the C(1–4) and C(8–11) fragments actually contrasts with the situations for other open ferrocenes, including Fe(2,4-C_7H_{11}), Fe(2,3,4-C_8H_{13})$_2$, and Fe(c-C_8H_{11})$_2$. It seems possible that this could be brought about by the particular edge bridge in this case, which is notably asymmetric. Thus, the C3–C2–C1–C7 and C10–C9–C8–C14 torsion angles average 53.8° versus 46.8° for their C3–C4–C5–C6 and C15–C11–C12–C13 counterparts. This leads to an even larger difference in the C2–C1–C7–C6 and C9–C8–C14–C13 versus C4–C5–C6–C7 and C11–C12–C13–C14 torsion angles, 35.9° versus 91.0°, respectively. This asymmetry is likely favored by the avoidance of eclipsing orientations of the hydrogen atoms on C6 and C7 [24]. Although there are additional parameters which deserve discussion, this must be postponed until publication of the structural details of Fe(6,6-dmch)$_2$.

2.2. Mössbauer spectroscopy

The gamma ray resonance spectra of the neutral compounds consist of two well separated components. From such spectra it is possible to extract the isomer shift (IS), related to the electron density around the metal atom nucleus, the quadrupole splitting (QS), related to the symmetry of the charge distribution around the metal atom, and the recoil-free fraction (f_a), related to the mean-square-amplitude of vibration (msav) of the metal atom. In addition, the temperature dependencies of these parameters, as well as the anisotropy of the msav (Gol'danskii–Karyagin effect) can be elucidated from a series of spectra at different temperatures. The values of these parameters and their significance will be discussed for the individual compounds in the following section.

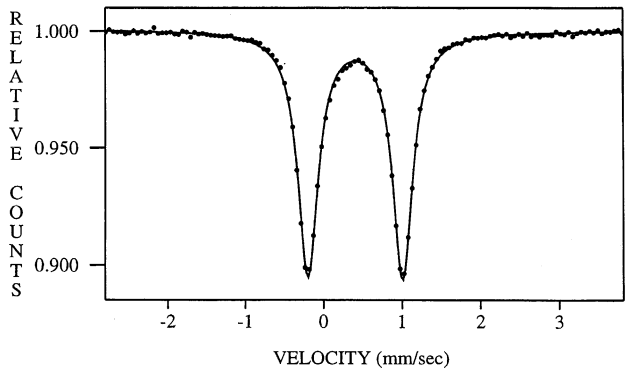

Fig. 3. Mössbauer spectrum of Fe(c-C_7H_9)$_2$ at 110 K. The velocity scale is defined relative to the centroid of a α-Fe spectrum at room temperature.

2.2.1. Bis(cycloheptadienyl)iron

A typical resonance spectrum of Fe(c-C_7H_9)$_2$ is shown in Fig. 3, and the IS and QS parameters at 90 K are summarized in Table 3. The IS at 90 K is significantly smaller than that previously reported [25] for neutral ferrocenoid iron complexes, as well as for the bis pentadienyl complexes previously discussed by Ernst et al. [11]. The smaller IS implies a larger s-electron density at the metal atom nucleus, suggesting that a larger ligand–metal interaction is obtained in the heptadienyl compound. The temperature dependence of the IS is not well represented by a linear regression, and the data show significant curvature over the temperature range $90 \leq T \leq 320$ K; hence it is not possible to extract a meaningful value of the effective vibrating mass, M_{eff} [26], from these results, in contrast to data to be discussed below. The QS shows a modest decrease with increasing temperature, consistent with the effects of thermal expansion as discussed earlier [27]. The temperature dependence of f_a — as extracted from the T-dependent area under the resonance curve — is summarized graphically in Fig. 4 which evidences a reasonably linear behavior at low temperatures, but departs from this linearity at $T > \sim 270$ K. Since this compound has a reported [12,28] T_{MP} of 364 ± 1 K, these observations imply a large increase in the msav of the iron atom (on warming) at temperatures well below the melting point. This type of behavior has been observed [29] in other ferrocene related solids, and can be associated with the onset of ring motion in these matrices. A differential scanning calorimetry study shows a sharp endotherm (on warming) at 326 K, and a smaller one at 330 K, as well as an exotherm (on cooling) at 274 K, consistent with the Mössbauer data of Fig. 4.

2.2.2. Bis(6,6′-dimethylcyclohexadienyl)iron

The synthesis and plausible structure based on IR inferences of Fe(6,6-dmch)$_2$ have been discussed by DiMauro and Wolczanski [13], who proposed an *anti*-eclipsed C_{2h} geometry in accord with calculations by Gleiter and coworkers [30]. The IS and QS parameters for this compound are included in Table 3 in addition to the other parameters extracted from the Mössbauer data, and are unexceptional. The IS is nearly linear over the whole temperature range (90–305 K) and is shown in Fig. 5. Above 150 K, the slope, d(IS)/dT, is $-(4.20 \pm 0.09) \times 10^{-4}$ mm s^{-1} K^{-1}, with a correlation coefficient of 0.997 for 17 data points, from which

Table 3
Summary of Mössbauer data for the compounds discussed in the text

Compound	IS(90) (mm s^{-1})	QS(90) (mm s^{-1})	$-d(IS)/dT$ (mm s^{-1} $K \times 10^4$)	M_{eff} (Da)	$-d\ln(A)/dT$ ($K^{-1} \times 10^3$)	θ_M (K)
$Fe(C_5H_5)_2$	0.531(3)	2.419(1)	3.29(7)	126	8.50(42)	85
$Fe(C_5Me_5)_2$	0.492(3)	2.473(17)	3.17(13)	131	7.97(40)	86
$Fe(C_5H_7)_2$ [a]	0.475(10)	1.402(15)	3.52	118(9)	5.13(22)	113(7)
$Fe(2\text{-}C_6H_9)_2$ [a]	0.458(5)	1.206(18)	3.84	108(9)	7.29(35)	99(7)
$Fe(3\text{-}C_6H_9)_2$ [a]	0.478(5)	1.255(41)	4.06	103(8)	5.49(41)	117(11)
$Fe(2,3\text{-}C_7H_{11})_2$ [a]	0.457(5)	1.261(6)	2.30	182(15)	7.94(46)	73.5
$Fe(2,4\text{-}C_7H_{11})_2$ [a]	0.494(7)	1.516(10)	3.60	116(9)	5.48(25)	111
$Fe(2,3,4\text{-}C_8H_{13})_2$	0.465(7)	1.404(5)	4.04	104(5)	7.22(20)	102
$Fe(6,6\text{-dmch})_2$	0.488(1)	1.143(1)	3.58(11) [b], 4.38(15) [c]	116 [b], 95 [c]	6.52(36) [d]	112 [e]
$Fe(c\text{-}C_7H_9)_2$	0.409(3)	1.207(1)	Not linear		5.89(28)	
$Fe(c\text{-}C_8H_{11})_2$	0.452(1)	1.535(1)	4.13(15)	100	7.20(26)	103
$Fe(C_5H_5)(2,4\text{-}C_7H_{11})$	0.470(5)	1.946(10)	3.09	111(8)	5.41(35)	103
$Fe(6,6\text{-dmch})_2^+$	0.578 [f], 0.457 [g]	0.892 [f], 0.878 [g]	6.4		[h]	
$Fe(C_5H_5)_2^+$	~0.4	0.1–0.6				

[a] Data from Ref. [11], corrected to 90 K.
[b] 90–298 K.
[c] 150–298 K.
[d] 90–190 K.
[e] From high T slopes.
[f] At 110 K.
[g] At 300 K.
[h] Spin–spin relaxation is fast even at 90 K.

M_{eff} is calculated to be 99 Da. The difference between M_{eff} and the 'bare' atom mass of 57 Da is due to the covalency of the Fe–ligand interaction. In this context, it should be noted that Brougham et al. [31], in their NMR and Mössbauer study of cyclohexadienyl and cycloheptadienyl complexes of the $Fe(CO)_3$ fragment, report $M_{eff} = 109$ and 117 Da, respectively, although (as noted by these authors) these values are based only on 78 and 295 K data — see footnotes b and c of Table 3.

The temperature dependence of the area under the resonance curve, $d(\ln A)/dT$, is shown graphically in Fig. 6. At low temperatures this dependence is nearly linear, but deviates dramatically from this dependence at temperatures above ~270 K, and becomes experimentally unobservable at temperatures above ~305 K. This T-dependence is completely reversible since the warming regime data (open circles) and cooling regime data (filled circles) are essentially superimposable. As Brougham et al. have noted from their solid state NMR data of the tri(carbonyl)iron complexes, there is a phase transition between 253 and 263 K, and 329 and 341 K, respectively, for the two complexes studied by them. They ascribe these transitions to the onset of ring rotation, and it is probable that the recoil-free fraction behavior shown in Fig. 6 is, in fact, a reflection of a similar kind of ring motion, which dramatically increases the msav of the iron atom in $Fe(6,6\text{-dmch})_2$, and hence leads to a marked decrease in the resonance effect above ~305 K.

2.2.3. Bis(6,6′-dimethylcyclohexadienyl)iron cation

A typical Mössbauer spectrum of $Fe(6,6\text{-dmch})_2^+$ at 110 K is shown in Fig. 7 and hyperfine parameters at 90 K are included in Table 3. The spectrum is characterized by two broad resonance lines of unequal intensity. Such spectra arise from relaxation effects involving the paramagnetic metal center. In contrast to other ferrocenium complexes reported [32] in the literature, which show a strong temperature dependence of the hyperfine and relaxation parameters, in the case of $Fe(6,6\text{-dmch})_2^+$ the spectra are insensitive to T over the range $90 \leq T \leq 300$ K. This observation leads to the conclusion that the paramagnetic relaxation is of the spin–spin type (rather than spin–lattice relaxation as was inferred for the ferrocenium complexes reported

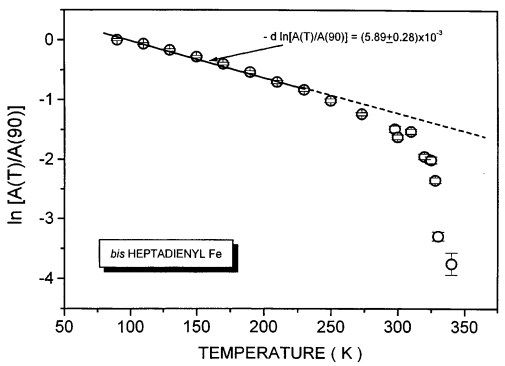

Fig. 4. Logarithm of the area under the resonance curve for $Fe(c\text{-}C_7H_9)_2$ as a function of temperature.

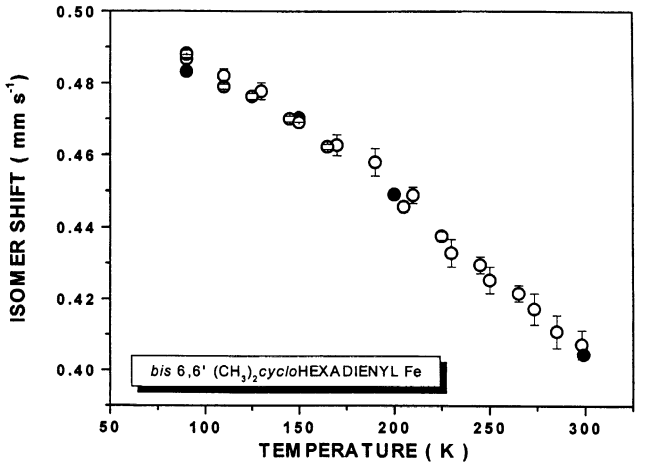

Fig. 5. Temperature dependence of the isomer shift for Fe(6,6-dmch)$_2$. The open circles refer to the warming regime, the closed circles to the cooling regime, illustrating the reversibility of the spectral data.

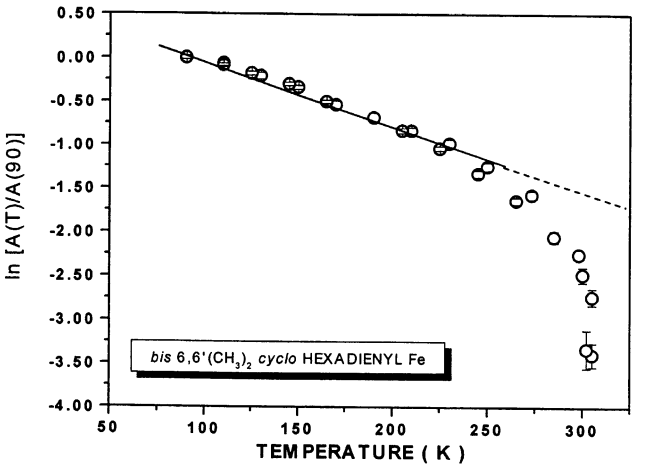

Fig. 6. Logarithm of the area under the resonance curve for Fe(6,6-dmch)$_2$ as a function of temperature. The straight line is meant as a guide.

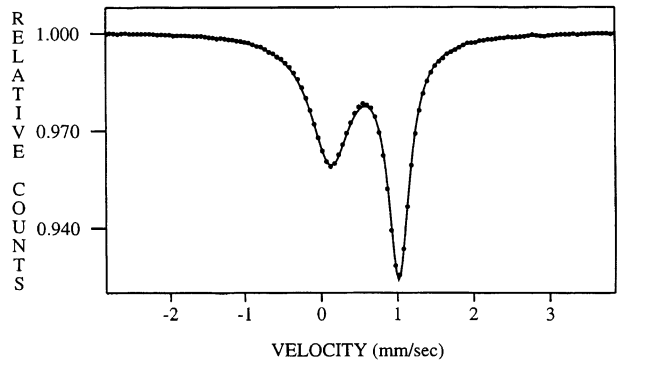

Fig. 7. Mössbauer spectrum of Fe(6,6-dmch)$_2^+$ at 110 K. The velocity scale is defined relative to the centroid of a α-Fe spectrum at room temperature.

earlier [32b]), and that this relaxation is fast on the Mössbauer time scale, even at 90 K.

2.2.4. Bis(cyclooctadienyl)iron

The hyperfine parameters of Fe(c-C_8H_{11})$_2$ at 90 K and the parameters derived therefrom are included in Table 3 from which it is noted that the IS(90) is intermediate between those of its six- and seven-membered ring analogues, while the QS(90) is significantly larger than that reported for the other open sandwich compounds of this study. Both the IS and ln(A) values are reasonably well represented by a linear regression over the temperature range $90 \leq T \leq 300$ K, permitting a calculation of $M_{\text{eff}} = 100$ Da, and a lattice temperature [26], $\theta_{\text{M}} = 103$ K. The latter value is comparable to that calculated for Fe(6,6-dmch)$_2$ (vide supra) and other related iron organometallics, and justifies the use of the 'high temperature' approximation in the calculation of M_{eff}. The QS parameter has a negative slope over the above temperature interval, as expected from covalent solid thermal expansion considerations, and none of the present data [IS(T), QS(T), and ln($A(T)$)] indicate evidence for any phase transitions over this interval. It is interesting to note in this context that in the iron tricarbonyl complexes reported by Brougham et al. [31], the onset of the ring re-orientation in the heptadienyl complex occurs some 76–78° higher than it does in the hexadienyl homologue. The same relative order may also obtain in the case of Fe(6,6-dmch)$_2$ and Fe(c-C_8H_{11})$_2$ (whether in solid or solution [24] state), but in the absence of high temperature (>300 K) Mössbauer data for the latter complex this conclusion must, at the present time, be considered speculative.

A number of interesting correlations may be drawn from the IS and QS values. First, for the neutral complexes one can observe that the IS values for the pentadienyl compounds are all significantly smaller than the value for ferrocene, reflecting a greater s electron density at the iron nuclei in the pentadienyl complexes. This trend can be attributed readily to the greater electron withdrawing ability of pentadienyl ligands, which would lead to greater positive charge on their iron centers, thereby causing a contraction of the metal orbitals, and greater s-electron density. Similarly, the neutral pentadienyl compounds are characterized by much lower QS values relative to ferrocene, a difference which has been attributed to a much higher degree of metal–ligand orbital mixing [8]. Theoretical studies indeed reveal enhanced metal–ligand mixing for pentadienyl [9,30,33], and the resulting increases in d_{xz} and d_{yz} orbital populations, and decreases in d_{xy} and $d_{x^2-y^2}$ populations, can clearly account for the substantial decreases in the QS values. Concerning the greater metal–pentadienyl orbital mixing, two mechanisms can be considered, one being the inherent differences in ligand orbital energies. In addition, however, it may be possible that the lower symmetry of the open fer-

rocenes, ideally C_2 versus at least D_5 for ferrocene, could actually be responsible. A distinction between these possibilities can be made using the QS data for the half-open ferrocene, $Fe(C_5H_5)(2,4\text{-}C_7H_{11})$. Should the orbital mixings be driven by the relative ligand orbital energies, one would expect this compound to have a QS value intermediate between those of ferrocene and $Fe(2,4\text{-}C_7H_{11})_2$. On the other hand, should symmetry be dominant, one would expect this low symmetry (C_s) compound to be characterized by a QS value similar to that of $Fe(2,4\text{-}C_7H_{11})_2$. That the QS value for the half-open ferrocene is almost exactly equal to the average of the QS value for ferrocene and $Fe(2,4\text{-}C_7H_{11})_2$ can be taken as a clear indication that it is the inherent ligand orbital energies, rather than the compound symmetries, which are important. Thus, the lower degree of resonance stabilization for pentadienyl versus Cp anions leads to the former having, on average, higher energy filled orbitals, which then serve as better electron donors, and lower energy empty orbitals, which then serve as better electron acceptors.

Although the general reductions in IS and QS values for the pentadienyl compounds may readily be accounted for, the differences in values for individual pentadienyl compounds generally seem to defy explanation. One does see an increase in QS value for the edge-bridged open ferrocenes as the bridge becomes longer, but their IS values follow no such trend. Similar confusing differences are found for the other open ferrocenes upon the addition of methyl groups in various locations (Table 3).

A final point of interest relates to the effects of oxidation on the IS and QS values. While oxidation of ferrocene leads to a small decrease in the IS value, attributable to a contraction of the metal s orbitals [34], one observes just the opposite change from the oxidation of $Fe(6,6\text{-dmch})_2$. Although it is possible that an increased degree of ligand-to-metal σ donation could lead to the higher s electron density, it would be desirable to have some theoretical substantiation for such a proposal. Concerning the QS value, oxidation of $Fe(6,6\text{-dmch})_2$ led to a small but noticeable decrease, whereas for ferrocene oxidation led to nearly a complete collapse of the QS value — from ca. 2.4 mm s^{-1} to ca. 0.1–0.6 mm s^{-1}, depending on the counterion. As a result, $Fe(6,6\text{-dmch})_2^+$ provides the only example in which an open ferrocene actually possesses a higher QS value than the ferrocene analogue itself. It would certainly be of interest to compare the changes in iron d orbital populations that accompany the oxidation of $Fe(6,6\text{-dmch})_2$ with the corresponding changes that occur for ferrocene, and it is hoped that appropriate studies along these lines will be pursued shortly.

3. Conclusions

The Mössbauer and structural data reported herein have provided some interesting insights into the differences in bonding for Cp and pentadienyl ligands. First, much lower quadrapole splitting values were observed for the 18 electron pentadienyl complexes as compared to ferrocene, which provides credible confirmation of theoretical results indicating much greater covalency (metal–ligand orbital mixing) for the open ligands. Furthermore, the fact that the QS value for the half-open ferrocene was found to be intermediate between those of ferrocene and $Fe(2,4\text{-}C_7H_{11})_2$ has allowed us to attribute the greater covalency to inherent ligand orbital energy differences rather than to a symmetry effect. While the greater orbital mixing in the open ferrocenes would be expected to lead to stronger Fe–ligand bonding, earlier structural data for $Fe(2,4\text{-}C_7H_{11})_2$ were not in accord with this view, an observation that had been ascribed to both steric and overlap problems for open dienyl bonding with the small iron center [7,8]. The fact that the structural data for $Fe(C_5H_5)(2,4\text{-}C_7H_{11})$ reveal nearly identical Fe–C distances for the two ligands confirms this conclusion, especially considering that for earlier metal analogues there is a clear structural preference for the open ligands [10].

Mössbauer data for the edge-bridged compounds have demonstrated that these species are also characterized by greater metal–ligand orbital mixings than ferrocene. The presence of edge bridges in these compounds has, however, been found to lead to profound differences relative to the non-bridged open ferrocenes, including the alteration of conformational preferences, and apparent ligand rotation even in the solid state, possibly as a result of the stabilization of the as yet unobserved *anti*-eclipsed conformation. The presence of an edge bridge has also been found to allow for the isolation of the first 17 electron open ferrocene cation, whose Mössbauer parameters suggest interesting electronic properties. While the current studies have therefore provided answers to some fundamental questions concerning these compounds, there clearly remain a number of additional issues that need to be addressed, especially for the $Fe(dmch)_2$ cation, and efforts along these lines are continuing.

4. Experimental

All reactions were carried out under N_2 atmosphere in Schlenk apparatus. Ether and hydrocarbon solvents were distilled from sodium–benzophenone under N_2 atmosphere. Published procedures were employed for the synthesis of 1,3-cycloheptadiene [35] and $Fe(c\text{-}C_8H_{11})_2$ [14], while $K(c\text{-}C_7H_9)$ was prepared according

to a general method for pentadienyl anions [36]. Elemental analysis was obtained from E and R Laboratory. Single crystals of $Fe(C_5H_5)(2,4\text{-}C_7H_{11})$ and $Fe(c\text{-}C_7H_9)_2$ were obtained by slowly cooling concentrated hydrocarbon solutions to -30 °C. Conditions for their X-ray data collections are summarized in Table 4. Both structures were solved straightforwardly using direct methods, and subsequent difference Fourier maps revealed all remaining atoms. Methyl group hydrogen atom locations were idealized, while the coordinates of all other hydrogen atoms were refined. All calculations employed the SHELXTL program package, and additional structural details may be obtained from the Cambridge Crystallographic Data Centre (see Section 5).

Mössbauer spectra were acquired and evaluated as described previously [23a,25,27], using a ~ 50 mCi source of $^{57}Co(Rh)$ in conjunction with a fast proportional counter and associated electronics. Typically an excess of 10^6 counts per channel (of 256) was acquired at each temperature, which was held constant to ± 0.5 K. All IS are reported with respect to the centroid of an α-Fe spectrum at room temperature (r.t.), which was also used to calibrate the velocity scale. The DSC data referred to in the text were acquired at heating (cooling) rates of 5 K min^{-1} using a Mettler Toledo Model DSC30 differential scanning calorimeter.

Table 4
Crystal data and structure refinement parameters for $Fe(C_5H_5)(2,4\text{-}C_7H_{11})$ and $Fe(c\text{-}C_7H_9)_2$.

Empirical formula	$FeC_{12}H_{16}$	$FeC_{14}H_{18}$
Formula weight	216.10	242.13
Crystal system	Orthorhombic	Triclinic
Space group	*Pnma*	$P\bar{1}$
Unit cell dimensions		
a (Å)	5.9428(2)	13.8790(4)
b (Å)	13.1192(7)	14.1131(3)
c (Å)	12.7727(6)	15.0322(5)
α (°)	90	62.0902(14)
β (°)	90	63.0398(9)
γ (°)	90	89.3141(16)
V (Å^3)	995.82(8)	2242.99(11)
Z	4	8
Crystal color, habit	Red prism	Red–orange prism
Crystal size (mm)	$0.20 \times 0.13 \times 0.10$	$0.26 \times 0.23 \times 0.14$
Temperature (K)	200	200
Diffractometer	Nonius Kappa CCD	Nonius Kappa CCD
Radiation λ (Å)	0.71073	0.71073
Data collected	3161	15 620
Observed unique data	1784	13 032
$R(F)$ [a]	0.0320	0.0373 (2σ)
$R(wF^2)$ [a]	0.0720	0.0767

[a] Quantity minimized $= R(wF^2) = \Sigma[w(F_o^2 - F_c^2)^2]/\Sigma[(wF_o^2)^2]^{1/2}$; $R = \Sigma\Delta/\Sigma(|F_o|)$, $\Delta = |(|F_o| - |F_c|)|$.

4.1. Bis(cycloheptadienyl)iron, $Fe(c\text{-}C_7H_9)_2$

This compound has previously been obtained from the reduction of $FeCl_3$ by a Grignard reagent in the presence of 1,3-cycloheptadiene [12]. The following alternative approach requires less diene and leads to higher yields of product. To a slurry of $FeCl_2$ (0.458 g, 3.61 mmol) in 30 ml of THF at -78 °C was slowly added a solution of $K(c\text{-}C_7H_9)$ (1.40 g, 10.8 mmol) in THF. After the addition was complete, the solution was allowed to warm to r.t. and was then stirred for 2 h. The solvent was removed in vacuo, leaving a dark brown residue, which was extracted using ca. 60 ml of hexane. The solution was filtered through a Celite pad on a coarse frit. The product was crystallized by concentration of the orange–brown filtrate in vacuo to ca. 20 ml and placement into a -30 °C freezer. After removal of the supernatant from the crystalline product, sublimation (50 °C, 10^{-2} Torr) afforded 420 mg (48% yield) of orange–red crystals. Spectroscopic data were consistent with those published previously [12].

4.2. Bis(6,6-dimethylcyclohexadienyl)iron tetraphenylborate, $[Fe(6,6\text{-}Me_2C_6H_5)_2]^+[B(C_6H_5)_4]^-$

To a solution of $Fe(6,6\text{-}Me_2C_6H_5)_2$ ([13], 200 mg, 0.740 mmol) in 20 ml of THF under N_2 at 0 °C was added solid $[Fe(C_5H_5)_2]BF_4$ [37] (200 mg, 0.731 mmol). Within a few minutes a green solution had resulted. After the solution had been stirred for 2 h, the solvent was removed in vacuo. The green residue was washed with pentane to remove ferrocene, and thereafter 20 ml of THF was added to the green residue, along with solid $NaB(C_6H_5)_4$ (250 mg, 0.730 mmol). After further stirring for 2 h at 0 °C the product had precipitated from the solution, and it was then collected by filtration through a coarse frit. The solid green product was dissolved in ca. 20 ml of MeCN. The product could be crystallized at -20 °C. After removal of the supernatant, the compound was dried in vacuo and isolated as a green crystalline solid (0.24–0.28 g, 55–65% yield). Anal. Found: C, 81.22; H, 7.34. Calc. for $C_{40}H_{42}BFe$: C, 81.51; H, 7.18%.

4.3. (Cyclopentadienyl)(2,4-dimethylpentadienyl)iron, $Fe(C_5H_5)(2,4\text{-}C_7H_{11})$

This compound was prepared as previously described [16]. Anal. Found: C, 66.79; H, 7.54. Calc. for $C_{12}H_{16}Fe$: C, 66.70; H, 7.46%.

^{1}H-NMR (benzene-d_6, ambient): δ 5.19 (s, 1H), 3.88 (s, 5H), 2.57 (s, 2H), 1.76 (s, 6H), -0.76 (s, 2H).

^{13}C-NMR (benzene-d_6, ambient): δ 93.1 (d, $J = 160$ Hz), 90.8 (s), 75.6 (d, Cp, $J = 176$ Hz), 43.5 (t, $J = 155$ Hz), 27.2 (q, $J = 127$ Hz).

EIMS (17 eV); m/z (relative intensity): 216 (27), 215 (15), 214 (100), 148 (33), 134 (15), 121 (33), 56 (43).

5. Supplementary material

Crystallographic data for structural analysis have been deposited with the Cambridge Crystallographic Data Centre, CCDC nos. 153826 and 153827 for compounds $Fe(C_5H_5)(2,4\text{-}C_7H_{11})$ and $Fe(c\text{-}C_7H_9)_2$. Copies of this information may be obtained free of charge from The Director, CCDC, 12 Union Road, Cambridge, CB2 1EZ, UK (Fax: +44-1223-336033; e-mail: deposit@ccdc.cam.ac.uk or www.ccdc.cam.ac.uk).

Acknowledgements

Partial support of this research by the NSF and University of Utah is gratefully acknowledged. We would like to thank Mr Bob LeSuer and Professor William Geiger for information and suggestions regarding the stability of the $Fe(dmch)_2$ cation.

References

[1] (a) A. McKnight, R.M. Waymouth, Chem. Rev. 88 (1988) 2587; (b) M. Bochmann, J. Chem. Soc. Dalton Trans. (1996) 255; (c) H.-H. Brintzinger, D. Fischer, R. Mülhaupt, B. Rieger, R.M. Waymouth, Angew. Chem. Int. Ed. Engl. 34 (1995) 1143; (d) D. Veghini, L.M. Henling, T.J. Burkhardt, J.E. Bercaw, J. Am. Chem. Soc. 121 (1999) 564; (e) F.J. Karol, C. Wu, W.T. Reichle, N.J. Maraschin, J. Catal. 60 (1979) 68.
[2] (a) A. Toqni, Angew. Chem. Int. Ed. Engl. 35 (1996) 1475; (b) in: A. Toqni, T. Hayashi (Eds.), Ferrocenes. Homogeneous Catalysis, Organic Synthesis, Materials Science, Weinheim, VCH, 1995.
[3] H. Schottenberger, K. Wurst, M.R. Buchmeiser, J. Organomet. Chem. 584 (1999) 301 (and references therein).
[4] J.A. Raloff, Sci. News 144 (1993) 223.
[5] D. Seyferth, A. Davison, Science 182 (1973) 699.
[6] (a) A. Haaland, Acc. Chem. Res. 12 (1979) 415; (b) A. Toqni, R. Halterman (Eds.), Metallocenes. Synthesis, Reactivity, Applications, vol. 1 and 2, VCH, Weinheim, 1998.
[7] (a) R.D. Ernst, Acc. Chem. Res. 18 (1985) 56; (b) R.D. Ernst, Struct. Bonding (Berlin) 57 (1984) 1.
[8] R.D. Ernst, Chem. Rev. 88 (1988) 1255.
[9] I. Hyla-Kryspin, T.E. Waldman, E. Meléndez, W. Trakarnpruk, A.M. Arif, M.L. Ziegler, R.D. Ernst, R. Gleiter, Organometallics 14 (1995) 5030.
[10] R.D. Ernst, Comments Inorg. Chem. 21 (1999) 285.
[11] R.D. Ernst, D.R. Wilson, R.H. Herber, J. Am. Chem. Soc. 106 (1984) 1646.
[12] J. Müller, B. Mertschenk, Chem. Ber. 105 (1972) 3346.
[13] P.T. DiMauro, P.T. Wolczanski, Organometallics 6 (1987) 1947.
[14] V. Kulsomphob, R. Tomaszewski, G.P.A. Yap, L.M. Liable-Sands, A.L. Rheingold, R.D. Ernst, J. Chem. Soc. Dalton Trans. (1999) 3995.
[15] P.T. DiMauro, P.T. Wolczanski, Polyhedron 14 (1995) 149.
[16] R. LeSuer, W.E. Geiger, unpublished results.
[17] Ch. Elschenbroich, E. Bilger, R.D. Ernst, D.R. Wilson, M.S. Kralik, Organometallics 4 (1985) 2068.
[18] (a) S. Carter, J.N. Murrell, J. Organometal. Chem. 192 (1980) 399; (b) D.L. Clark, J.C. Gordon, J.T. McFarlan, R.L. Vincent-Hollis, J.G. Watkin, B.D. Zwick, Inorg. Chim. Acta 244 (1996) 269.
[19] (a) R.K. Bohn, A. Haaland, J. Organomet. Chem. 5 (1966) 470; (b) A. Haaland, J.E. Nilsson, Acta Chem. Scand. 22 (1968) 2653.
[20] The first value in parenthesis represents the variation in values being averaged, while the second value represents the uncertainty in the average value.
[21] D.R. Wilson, R.D. Ernst, T.H. Cymbaluk, Organometallics 2 (1983) 1220.
[22] (a) R. Hoffmann, P. Hofmann, J. Am. Chem. Soc. 98 (1976) 598; (b) R.D. Ernst, T.H. Cymbaluk, Organometallics 1 (1982) 708.
[23] (a) J.-C. Han, J.P. Hutchinson, R.D. Ernst, J. Organomet. Chem. 321 (1987) 389; (b) W. Trakarnpruk, A.M. Arif, R.D. Ernst, J. Organomet. Chem. 485 (1995) 25.
[24] D.A. Brown, N.J. Fitzpatrick, M.A. McGinn, J. Chem. Soc. Dalton Trans. (1986) 701.
[25] (a) R.H. Herber, I. Gattinger, F.H. Köhler, Inorg. Chem. 39 (2000) 851; (b) R.H. Herber, B. Bildstein, P. Denifl, H. Schottenberger, Inorg. Chem. 36 (1997) 3586 (and references therein).
[26] R.H. Herber, in: R.H. Herber (Ed.), Chemical Mössbauer Spectroscopy, Plenum Press, New York, 1984, pp. 199–216.
[27] R.H. Herber, Inorg. Chim. Acta 291 (1999) 74.
[28] E.O. Fischer, J. Müller, J. Organomet. Chem. 1 (1963) 89.
[29] (a) R.H. Herber, I. Nowik, Hyperfine Interact. 126 (2000) 127; (b) H. Schottenberger, M.R. Buchmeiser, R.H. Herber, J. Organomet. Chem. 612 (2000) 1.
[30] (a) M.C. Böhm, M. Eckert-Maksić, R.D. Ernst, D.R. Wilson, R. Gleiter, J. Am. Chem. Soc. 104 (1982) 2699; (b) R. Gleiter, M.C. Böhm, R.D. Ernst, Electron. Spectrosc. Relat. Phenom. 22 (1984) 269.
[31] D.F. Brougham, P.J. Barrie, G.E. Hawkes, I. Abramams, M. Motevalli, D.A. Brown, G.J. Long, Inorg. Chem. 35 (1996) 5595.
[32] (a) R.J. Webb, M.D. Lowery, Y. Shiomi, M. Sorai, R.J. Wittebort, D.N. Hendrickson, Inorg. Chem. 31 (1992) 5211 (and references therein); (b) R.H. Herber, T.P. Hanusa, Hyperfine Interact. 108 (1997) 563.
[33] R.M. Kowaleski, F. Basolo, J.H. Osborne, W.C. Trogler, Organometallics 7 (1988) 1425.
[34] R.H. Herber, in: M. Tsutsui (Ed.), Characterization of Organometallic Compounds. Part 1, Interscience, New York, 1969, p. 326ff.
[35] A.P. Ter Borg, A.F. Bickel, Recueil 80 (1961) 1229.
[36] D.R. Wilson, L. Stahl, R.D. Ernst, Organomet. Synth. 3 (1986) 136.
[37] D.N. Hendrickson, Y.S. Sohn, H.B. Gray, Inorg. Chem. 10 (1971) 1559.